

Higher charge periodic monopoles

Rafael Maldonado*

*Department of Mathematical Sciences,
South Road, Durham DH1 3LE, UK*

August 18, 2021

Abstract

We consider singly periodic solutions to the $SU(2)$ Bogomolny equations and use the Nahm transform to generate a class of monopoles of charge $k > 2$, thereby extending known results for lower charge chains. Some simple scattering processes are presented and a comparison made with geodesic motion of monopoles in \mathbb{R}^3 .

1 Introduction

Solutions of the Bogomolny (monopole) equations on $\mathbb{R}^2 \times S^1$ were first considered by Cherkis & Kapustin [1, 2], where the Nahm transform was adapted to this topology. Approximate solutions of charge 1 and 2 were then constructed by Harland and Ward [3, 4], and a further class of charge 2 solutions was introduced in [5]. These charge 2 examples suggest an Ansatz for higher charge solutions, which will be presented in this paper. If the size to period ratio C is small, the results reproduce qualitatively the scattering processes described in [6, 7]. We will also consider the ‘spectral approximation’ of [5], which describes the limit of large C .

The structure of this paper is as follows. Section 2 describes the setup specific to this case and introduces the spectral curve used in the Nahm construction (the reader is referred to [5] for a more general formulation). In section 3 we give a charge 2 solution to the Nahm/Hitchin equations and show how it is generalised to arbitrary charge, considering the symmetries of the resulting monopole configurations. Section 4 extends a result of [3] to show that higher charge monopole chains can be constructed from lower charge chains by taking adjacent monopoles in pairs. We wrap up with some conclusions and ideas for further work.

*rafael.maldonado@durham.ac.uk

2 Setup

The periodic monopole can be constructed by use of a generalised Nahm transform, which maps between solutions of the SU(2) Bogomolny equations of charge k on $\mathbb{R}^2 \times S^1$, and rank k Hitchin data on the dual cylinder $\mathbb{R} \times S^1$. On the monopole side we define the complex coordinate $\zeta = \rho e^{i\theta}$ on \mathbb{R}^2 and $z \sim z + \beta$ on S^1 , while on the Nahm/Hitchin cylinder we define $r \in \mathbb{R}$ and $t \sim t + 2\pi/\beta$ which we combine into a complex coordinate $s = r + it$. The Hitchin equations

$$F_{s\bar{s}} = -\frac{1}{4}[\Phi, \Phi^\dagger] \quad D_{\bar{s}}\Phi = \partial_{\bar{s}}\Phi + [A_{\bar{s}}, \Phi] = 0$$

with \dagger denoting complex conjugate transpose are now to be solved for rank k matrix-valued fields, where the characteristic polynomial of Φ is determined by the spectral curve described in section 2.1. The monopole fields are recovered, up to a gauge, through solutions of the inverse Nahm equation,

$$\Delta\Psi = \begin{pmatrix} \mathbf{1}_k \otimes (2\partial_{\bar{s}} - z) + 2A_{\bar{s}} & \mathbf{1}_k \otimes \zeta - \Phi \\ \mathbf{1}_k \otimes \bar{\zeta} - \Phi^\dagger & \mathbf{1}_k \otimes (2\partial_s + z) + 2A_s \end{pmatrix} \Psi = 0 \quad (1)$$

where Ψ is a $(2k \times 2)$ matrix $(\Psi_+^\top \Psi_-^\top)^\top$, subject to the normalisation condition

$$\int_{-\infty}^{\infty} dr \int_{-\pi/\beta}^{\pi/\beta} dt (\Psi^\dagger \Psi) = \mathbf{1}_2.$$

One can then construct the monopole fields using

$$\hat{\Phi} = i \int_{-\infty}^{\infty} dr \int_{-\pi/\beta}^{\pi/\beta} dt (r \Psi^\dagger \Psi) \quad \hat{A}_i = \int_{-\infty}^{\infty} dr \int_{-\pi/\beta}^{\pi/\beta} dt (\Psi^\dagger \partial_i \Psi).$$

Gauge transformations \hat{g} acting on the monopole fields and g on the Nahm fields transform Ψ as

$$\Psi(s; \zeta, z) \mapsto U(s)^{-1} \Psi(s; \zeta, z) \hat{g}(\zeta, z),$$

a relation we will use to study the spatial symmetries of the monopole corresponding to a given solution of the Hitchin equations. Here, $U = h \otimes g(s)$ and h is a constant matrix serving to permute the entries of Δ and those of Ψ .

2.1 Spectral curve

The spectral curve of a periodic monopole was introduced by Cherkis & Kapustin [1, 2] where an equivalence was proven between the ‘monopole’ and ‘Hitchin’ spectral curves, which are polynomials of degree 2 in w and of degree k in ζ . The monopole spectral curve is the characteristic equation of the z -holonomy of the monopole fields, $\det(w - V(\zeta)) = 0$, where $w = e^{\beta s}$,

$$b_k \zeta^k + b_{k-1} \zeta^{k-1} + \cdots + b_1 \zeta + (b_0 + w + w^{-1}) = 0, \quad (2)$$

where the coefficients b_i are independent of s . The Hitchin spectral curve is defined from the Nahm data, through $\det(\zeta - \Phi) = 0$,

$$\zeta^k - \zeta^{k-1}\text{tr}(\Phi) + \dots + (-1)^k \det(\Phi) = 0.$$

By matching coefficients of powers of ζ we obtain the gauge invariants of Φ as a function of w and the moduli encoded by the $\{b_i\}$. It should be noted that the spectral curve only encodes half of the total number of expected moduli (for a centered chain the relative moduli space \mathcal{M}_k has real dimension $4k-4$). In [3] and [5] it was shown that in the charge $k = 2$ case the moduli present in the spectral curve provide a geodesic submanifold of \mathcal{M}_2 . These moduli describe the relative xy positions of the monopoles but are insensitive to a z offset and relative phase. For higher charges, however, the remaining moduli have yet to be identified. We appeal to the charge 2 result and assume that the moduli appearing in the spectral curve are the fixed point set of some symmetry group of the full moduli space, and thus describe a geodesic submanifold which, following [6], we denote by Σ_k^ℓ , where ℓ labels different such submanifolds.

It has been found [5] that an approximation to the monopole fields in the limit of large size to period ratio (in which the monopole fields are increasingly independent of z) can be read off the spectral curve polynomial (2) by expressing s in terms of ζ . We then have $\hat{\Phi} = i\text{Re}(s(\zeta))\sigma_3$, from which the energy density is calculated using

$$\mathcal{E} = \partial_\zeta \partial_{\bar{\zeta}} |\text{tr}(\hat{\Phi}^2)|.$$

We will use this result in the following sections to visualise monopole fields with various spatial symmetries.

2.2 Charge 3 symmetries

Geodesic submanifolds can be identified by considering the fixed point sets of symmetries of the spectral curve. We consider two transformations of ζ (corresponding to a rotation by α and a reflection in the line $\theta = \alpha/2$), and find the necessary maps of the coefficients b_i such that the original spectral curve is recovered. The $k = 3$ spectral curve can be written

$$w^2 + w(b_3\zeta^3 + b_2\zeta^2 + b_1\zeta + b_0) + 1 = 0. \quad (3)$$

We take $b_3 = 1$ for the rest of this section, its magnitude setting a scale and its phase an orientation. We also fix the centre of mass of the spectral points at the origin by setting $b_2 = 0$.

$$\zeta \mapsto \zeta e^{i\alpha}$$

To keep the spectral curve invariant we transform $w \mapsto w e^{-3i\alpha}$ and look for values of α for which the resulting spectral curve,

$$w^2 e^{-6i\alpha} + w(\zeta^3 + b_1 \zeta e^{-2i\alpha} + b_0 e^{-3i\alpha}) + 1 = 0,$$

is the same as the original one, (3), for a certain choice of b_1 and b_0 .

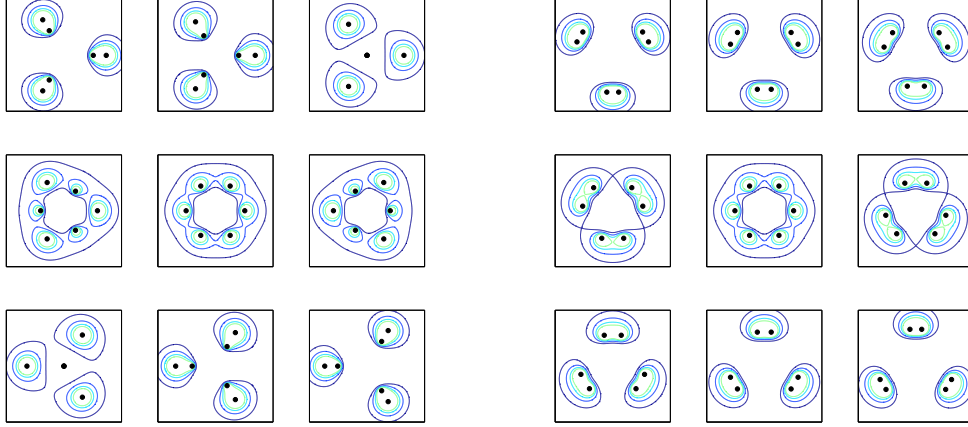


Figure 1: Cross section of energy density for two one-parameter families with $b_1 = 0$. Left, $b_0 \in \mathbb{R}$ with $b_0 \in [-4, 4]$. The relevant symmetries are i, ii, iv and vi in the list above. Right, $b_0 \in i\mathbb{R}$ with $-ib_0 \in [-4, 4]$, with symmetries i, ii, v and vii.

- i. $\alpha = \pi/3$, $b_1 \mapsto e^{2i\pi/3}b_1$, $b_0 \mapsto -b_0$, with fixed set $b_1 = b_0 = 0$. This corresponds to the hexagonally symmetric configuration of spectral points.
- ii. $\alpha = 2\pi/3$, $b_1 \mapsto e^{4i\pi/3}b_1$, $b_0 \mapsto b_0$, with fixed set $b_1 = 0$ for all b_0 .
- iii. $\alpha = \pi$, $b_1 \mapsto b_1$, $b_0 \mapsto -b_0$, with fixed set $b_0 = 0$ for all b_1 .

$$\zeta \mapsto \bar{\zeta}e^{i\alpha}$$

We also set $w \mapsto \bar{w}e^{-3i\alpha}$, such that

$$\bar{w}^2e^{-6i\alpha} + \bar{w}(\bar{\zeta}^3 + b_1\bar{\zeta}e^{-2i\alpha} + b_0e^{-3i\alpha}) + 1 = 0$$

$$w^2e^{6i\alpha} + w(\zeta^3 + \bar{b}_1\zeta e^{2i\alpha} + \bar{b}_0e^{3i\alpha}) + 1 = 0.$$

- iv. $\alpha = 0$, $b_1 \mapsto \bar{b}_1$, $b_0 \mapsto \bar{b}_0$, with fixed set $b_1 \in \mathbb{R}$ and $b_0 \in \mathbb{R}$.
- v. $\alpha = \pi/3$, $b_1 \mapsto e^{2i\pi/3}\bar{b}_1$, $b_0 \mapsto -\bar{b}_0$, with fixed set $b_1 = e^{i\pi/3}|b_1|$, $b_0 \in i\mathbb{R}$.
- vi. $\alpha = 2\pi/3$, $b_1 \mapsto e^{-2i\pi/3}\bar{b}_1$, $b_0 \mapsto \bar{b}_0$, with fixed set $b_1 = e^{-i\pi/3}|b_1|$, $b_0 \in \mathbb{R}$.
- vii. $\alpha = \pi$, $b_1 \mapsto \bar{b}_1$, $b_0 \mapsto -\bar{b}_0$, with fixed set $b_1 \in \mathbb{R}$ and $b_0 \in i\mathbb{R}$.

The above symmetries of the spectral curve can be combined to give three distinct scattering processes, described in figs 1 and 2.

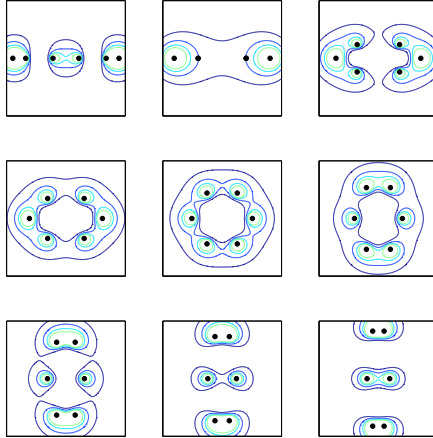


Figure 2: Energy density for $b_1 \in \mathbb{R}$, $b_0 = 0$, with $b_1 \in [-4, 4]$. Unlike the symmetries in fig. 1, this family does not have a charge 2 analogy, and in fact the Nahm data is only known for the special case $b_1 = -3$, $b_0 = 0$ (top middle picture). This configuration is in fact a charge 1 chain with period $\beta/3$ and is described in section 4.1. The relevant symmetries are i, iii, iv and vii.

3 Constructing solutions

We start this section by recalling the charge 2 solutions to the Nahm equations described in [3, 5], and then give an extension to higher charges, making specific reference to the charge 3 and 4 cases as an illustration.

3.1 Charge 2

For $k = 2$ the spectral curve polynomials require that the Hitchin Higgs field Φ is of rank 2 and satisfies

$$\mathrm{tr}(\Phi) = 0 \quad -\det(\Phi) = C \cosh(\beta s) - K/2$$

where C and K are defined in terms of the coefficients in (2) by $C = -2/b_2$ and $K = 2b_0/b_2$, such that C is fixed by the boundary conditions and describes the size and orientation of the monopole (we will take it to be real and positive) and K is a complex modulus encoding the positions of the monopoles in the xy plane. In [3] it was shown that the general solution to the Hitchin equations is (up to a gauge)

$$\Phi = \begin{pmatrix} 0 & \mu_+ e^{\psi/2} \\ \mu_- e^{-\psi/2} & 0 \end{pmatrix} \quad A_{\bar{s}} = a\sigma_3 + \alpha\Phi \quad A_s = -A_{\bar{s}}^\dagger,$$

where $4a = -\partial_{\bar{s}}\psi$,

$$\nabla^2 \mathrm{Re}(\psi) = 2(1 + 4|\alpha|^2) \left(|\mu_+|^2 e^{\mathrm{Re}(\psi)} - |\mu_-|^2 e^{-\mathrm{Re}(\psi)} \right)$$

and

$$e^{-\text{Re}(\psi)/2} \partial_s \left(\alpha \mu_+ e^{\text{Re}(\psi)} \right) + e^{\text{Re}(\psi)/2} \partial_{\bar{s}} \left(\bar{\alpha} \bar{\mu}_- e^{-\text{Re}(\psi)} \right) = 0.$$

Imposing that the monopole fields have the spatial symmetry $(\zeta, z) \sim (-\zeta, z)$ fixes $\alpha = 0$, as can be seen by gauge transforming the Hitchin fields by σ_3 along with $\Psi_{\pm} \mapsto \pm \Psi_{\pm}$ in the inverse Nahm operator (1). The function α is expected to encode the two remaining moduli: a z offset and relative phase.

The key point is that $C \cosh(\beta s) - K/2$ has two zeroes, whose positions depend on the value of K/C . There are then two classes of smooth solutions of the Hitchin equations, according to the allocation of zeroes between μ_+ and μ_- , such that $\ell = 0$ if both zeroes are in μ_+ and $\ell = 1$ if one is in each of μ_{\pm} (see section 2.1). Geodesics on each of these submanifolds are studied by transforming s and K in such a way that the transformed fields can be written as a gauge transformation of the original fields and then observing the effect of this change on the monopole coordinates ζ and z via (1) (for more details, see [5]).

- The $\ell = 0$ solution has

$$\mu_+ = C \cosh(\beta s) - K/2 \quad \mu_- = 1 \quad (4)$$

with $\text{Im}(\psi) = 0$. The geodesics $K \in \mathbb{R}$ and $K \in i\mathbb{R}$ describe $\pi/2$ scattering of monopoles in the xy plane, via a toroidal central configuration with discrete \mathbb{Z}_4 symmetry.

- The $\ell = 1$ configuration has

$$\mu_{\pm} = \sqrt{C/2} \left(e^{\beta s/2} - W^{\pm 1} e^{-\beta s/2} \right) \quad \text{with} \quad K/C = W + W^{-1} \quad (5)$$

and $\text{Im}(\psi) = -\beta t$ in order for Φ to be periodic with $t \sim t + 2\pi/\beta$. Simple geodesics representing monopole scattering are obtained as fixed points of the symmetries of the Hitchin equations, as described in [8] (note that [3, 5] interpret the branch structure differently). Two of them correspond to double scattering, first along z and then in the xy plane (either parallel or at right angles to the incoming monopoles), while $|W| = 1$ is a closed geodesic with monopoles fixed at $z = \pm\beta/4$ but oscillating in shape.

3.2 Higher charges

A straightforward extension of the charge 2 solutions described in the previous section is a modification of ‘‘Sutcliffe’s ansatz’’ [9, 10]. Solutions generated in this way have $b_i = 0$ for $i \neq 0, k$ in (2). We take

$$\Phi = \begin{pmatrix} 0 & 0 & \cdots & 0 & f_1 \\ f_2 & 0 & \cdots & 0 & 0 \\ 0 & f_3 & \cdots & 0 & 0 \\ \vdots & \vdots & \ddots & \vdots & \vdots \\ 0 & 0 & \cdots & f_k & 0 \end{pmatrix} \quad A_{\bar{s}} = \begin{pmatrix} a_1 & 0 & 0 & \cdots & 0 \\ 0 & a_2 & 0 & \cdots & 0 \\ 0 & 0 & a_3 & \cdots & 0 \\ \vdots & \vdots & \vdots & \ddots & \vdots \\ 0 & 0 & 0 & \cdots & a_k \end{pmatrix}. \quad (6)$$

Mimicking the charge 2 procedure, we define $f_i = \mu_i e^{\psi_i/2}$, with the conditions $\sum_{i=1}^k \psi_i = 0$ and $\prod_{i=1}^k \mu_i = (-1)^{k-1} \det(\Phi)$. The Hitchin equations then become

$$\begin{aligned} 2(a_{i-1} - a_i) &= \partial_{\bar{s}} \psi_i \\ \nabla^2 \log |f_i|^2 &= 2|f_i|^2 - |f_{i-1}|^2 - |f_{i+1}|^2 \end{aligned}$$

where the index i is periodic, such that $f_0 = f_k$. As was the case in section 3.1, the determinant of Φ has exactly two zeroes, such that smooth solutions must have both zeroes in the same or different entries μ_i (such that two of the μ_i are μ_{\pm} and all the others are set to 1). We are free to fix one of the zeroes, $\mu_1 = \mu_+$. Then for given charge k , the $\ell = 0$ configuration has both zeroes in μ_1 , and there are $(2k + (-1)^k - 1)/4$ gauge inequivalent configurations with $\ell > 0$, where ℓ is the separation between the positions of μ_{\pm} in Φ , so in particular $\mu_{1+\ell} = \mu_-$. With this notation, the Hitchin equations for $k = 3$, $\ell = 1$ are

$$\begin{cases} \nabla^2 \text{Re}(\psi_1) &= 2|\mu_+|^2 e^{\text{Re}(\psi_1)} - |\mu_-|^2 e^{\text{Re}(\psi_2)} - e^{-\text{Re}(\psi_1 + \psi_2)} \\ \nabla^2 \text{Re}(\psi_2) &= 2|\mu_-|^2 e^{\text{Re}(\psi_2)} - |\mu_+|^2 e^{\text{Re}(\psi_1)} - e^{-\text{Re}(\psi_1 + \psi_2)} \end{cases} \quad (7)$$

with μ_{\pm} as in (4) or (5).

Solving the Hitchin equations numerically is now a matter of adapting the charge 2 procedure used in [3]. First of all we note the equations (7) can be obtained by varying the functional

$$E[\text{Re}(\psi_i)] = \int dr dt \left(\frac{1}{2} \sum_{p=r,t} (\partial_p \text{Re}(\psi_i))^2 + 2|\mu_i|^2 e^{\text{Re}(\psi_i)} - \psi_i |\mu_j|^2 e^{\text{Re}(\psi_j)} + e^{-\text{Re}(\psi_i + \psi_j)} \right) \quad (8)$$

with respect to ψ_i , where $i, j \in \{1, 2 | i \neq j\}$ and no sum is implied. Unfortunately there appears to be no simple way of combining the two functionals which generate the separate equations (7) into a single expression. Instead of minimising a single functional, we alternately minimise $E[\text{Re}(\psi_1)]$ and $E[\text{Re}(\psi_2)]$. This approach was found to lead to rapidly convergent solutions as long as the boundary conditions were chosen appropriately. In fact, it is straightforward to write down an asymptotic solution to (7) valid away from the zeroes of μ_{\pm} by making the Ansatz $\psi_i = \log(|\mu_+|^{\nu_i^+} |\mu_-|^{\nu_i^-})$ and solving for the ν_i^{\pm} (this solution is singular at the zeroes of μ_{\pm} and is thus not globally valid). For $k = 3$ and $\ell = 1$ we find

$$\text{Re}(\psi_1) = \frac{2}{3} \log \frac{|\mu_-|}{|\mu_+|^2} \quad \text{Re}(\psi_2) = \frac{2}{3} \log \frac{|\mu_+|}{|\mu_-|^2} \quad \text{Re}(\psi_3) = \frac{2}{3} \log (|\mu_+| |\mu_-|).$$

There is some freedom in the choice of imaginary parts of the functions ψ_i , which must be chosen so as to make the Nahm data periodic on the cylinder. We fix $\text{Im}(\psi_1) = -\beta t$, $\text{Im}(\psi_{1+\ell}) = \beta t$ and $\text{Im}(\psi_3) = 0$. A different choice simply corresponds to a global shift in the z direction, and the resulting moduli space is isomorphic to Σ_3^1 .

One might also be concerned by the fact that (8) is not explicitly positive definite due to the term linear in ψ_i , which does not appear in the charge 2 case. We again resort to the convergence of the numerical solution to justify this approach.

It is easy to see that there are no solutions with $\text{Re}(\psi_1) = \text{Re}(\psi_2) = 0$ everywhere. This tells us that the charge 1 chain of period $\beta/3$ is not included in this family of solutions, as this would require $F = 0$ (see also section 4.1).

3.3 Symmetries

Spatial symmetries of the monopole fields can be studied by the procedure outlined in section 3.1. First of all we choose a transformation of K (or W) and s which preserves the spectral curve for a given transformation of ζ . Then we express the transformed Hitchin fields as a gauge transformation of the original fields. This allows us to read off the corresponding change in z from the inverse Nahm operator (1).

Note that if we restrict to gauge transformations which change the positions and phases of the entries of Φ , then the overall ordering of the f_i is unchanged (or reversed in the case of Φ^\dagger). This property gives the solutions $\ell = 0$ and $\ell = k/2$ (for k even) an additional $s \mapsto -s$ symmetry (corresponding to $z \mapsto -z$), which is not observed for general ℓ .

Various scattering processes generalising those in section 3.1 are described in the following subsections, and we visualise them with reference to chains of small monopoles ($C \lesssim 1$). In summary, it is found that the geodesics are characterised by the positions of the zeroes among the entries of Φ , say at f_1 and $f_{1+\ell}$. Then for $|W| > 1$ the monopoles are located on the vertices of a regular k -gon at $z = \beta\ell/k$ (the z position is determined numerically). As $|W|$ is reduced they scatter and split into two clusters of charge ℓ moving along the positive z axis and $(k-\ell)$ along the negative z axis. The clusters move at speeds inversely proportional to their charges, such that for $|W| < 1$ the outgoing monopoles emerge at $z = 0$ on a (possibly rotated) k -gon. Following the discussion of [8] we expect there to be a closed geodesic with $|W| = 1$, describing stationary monopoles oscillating in shape. A discussion of the motion of Higgs zeroes is given in section 3.4.

3.3.1 Planar scattering

The geodesic surface Σ_k^0 with $K \in \mathbb{R}$ or $K \in i\mathbb{R}$ describes scattering in the xy plane via a \mathbb{Z}_{2k} -symmetric toroidal configuration. We see this as follows:

First of all, note that under the transformation $s \mapsto -s$, μ_\pm and ψ are invariant and $a_i(s) \mapsto a_i(-s) = -a_i(s)$. The form of the inverse Nahm operator (1) now tells us that the monopole fields are invariant if we also replace z by $-z$. Thus, this monopole configuration has the symmetry $(\zeta, z) \sim (\zeta, -z)$, consistent with the k incoming monopoles being located at $z = 0$ (the fixed point set of this transformation).

To see the \mathbb{Z}_{2k} symmetry we perform the transformation $(s; K) \mapsto (s + i\frac{\pi}{\beta}; -K)$, giving $\mu_\pm \mapsto \mp\mu_\pm$ and $\psi_i \mapsto \psi_i$. Then $\Phi'(s, K) = \Phi(s + i\frac{\pi}{\beta}, -K)$ is the same as $\Phi(s; K)$ but with the sign of f_1 reversed. Under a suitably chosen diagonal gauge transformation g , we then have $\Phi' = e^{i\pi/k} g^{-1} \Phi g$, leaving A unchanged. The entry $(\zeta - \Phi)$ in the inverse Nahm operator (1) implies that $\zeta \mapsto \zeta e^{i\pi/k}$ when we map K to $-K$. The monopole fields are symmetric under $(\zeta, z; K) \mapsto (\zeta e^{i\pi/k}, z; -K)$, and thus $K = 0$ describes a configuration of enhanced symmetry.

3.3.2 Symmetric splitting

For even k , the geodesic submanifold $\Sigma_k^{k/2}$ describes a splitting of k incoming monopoles into two equal clusters. In the case of Σ_4^2 we identify the following symmetries:

- $(s, W) \mapsto (-\bar{s}, \bar{W}) \Rightarrow (\zeta, z) \mapsto (\bar{\zeta}, z)$, fixing the geodesic $W \in \mathbb{R}$.
- $(s, W) \mapsto (i\pi/\beta - \bar{s}, -\bar{W}) \Rightarrow (\zeta, z) \sim (e^{i\pi/4}\bar{\zeta}, z)$, with fixed point set $W \in i\mathbb{R}$.
- $(s, W) \mapsto (\bar{s}, \bar{W}^{-1}) \Rightarrow (\zeta, z) \mapsto (\bar{\zeta}, \beta/2 - z)$, relates the incoming and outgoing legs of the geodesics $W \in \mathbb{R}$ and $W \in i\mathbb{R}$. Thus, $W \in \mathbb{R}$ describes monopoles incoming and outgoing parallel to the x and y axes, with a half-period shift along z . On the other hand, $W \in i\mathbb{R}$ has an additional $\pi/4$ rotation about the z axis. This symmetry also fixes the closed geodesic $|W| = 1$.
- $(\zeta, z) \mapsto (i\zeta, z)$ is a symmetry for all W , as can be seen by the gauge transformation $g = \text{diag}(1, i, -1, -i)$.
- $s \mapsto -s \Rightarrow (\zeta, z) \mapsto (\zeta, -z)$ for all W .

There are two particularly symmetric cases which will be considered in more detail in section 4,

- $W = 1$ has $(\zeta, z) \sim (\zeta, \beta/2 - z) \sim (\zeta, z + \beta/2)$,
- $W = i$ has $(\zeta, z) \sim (e^{i\pi/4}\zeta, \beta/2 - z) \sim (e^{i\pi/4}\zeta, z + \beta/2)$.

The fixed points of these symmetries tell us that the clusters are located at $z = \pm\beta/4$.

3.3.3 Generic ℓ

Here we consider the example of Σ_3^1 . The symmetries are

- $(s, W) \mapsto (-\bar{s}, \bar{W}) \Rightarrow (\zeta, z) \mapsto (\bar{\zeta}, z)$, for $W \in \mathbb{R}$.
- $(s, W) \mapsto (i\pi/\beta - \bar{s}, -\bar{W}) \Rightarrow (\zeta, z) \sim (-\bar{\zeta}, z)$, for $W \in i\mathbb{R}$.
- $(s, W) \mapsto (\bar{s}, \bar{W}^{-1}) \Rightarrow (\zeta, z) \mapsto (\bar{\zeta}, \beta/3 - z)$.
- $(\zeta, z) \mapsto (e^{2i\pi/3}\zeta, z)$ is a symmetry for all W .

In this case, there is no symmetry $z \mapsto -z$ due to the asymmetric splitting. There are still points with enhanced symmetry,

- $W = 1$ has $(\zeta, z) \sim (\zeta, \beta/3 - z)$,
- $W = i$ has $(\zeta, z) \sim (-\zeta, \beta/3 - z)$,

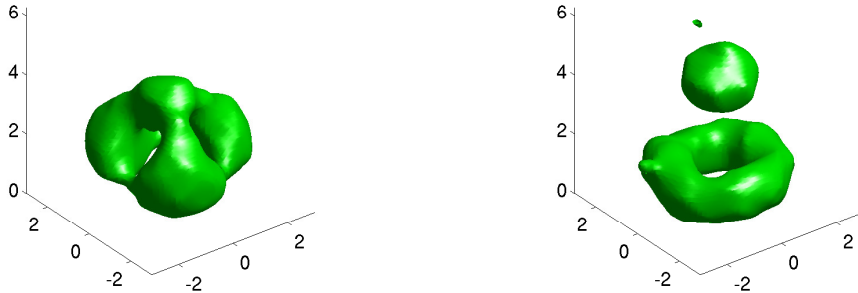


Figure 3: Energy density of a charge 3 periodic monopole with $C = 1$ taken over a single period. Left: approximately tetrahedral configuration with $W = 2 + \sqrt{3}$ ($K = 4$). Right: clusters of charge 1 and 2 are visible at $W = i$.

with fixed points at $z = \beta/6$ and $2\beta/3$, which are the positions of the charge 2 and charge 1 clusters.

These symmetries are consistent with the expected scattering process. Monopoles are incoming on the vertices of an equilateral triangle. They scatter along z via an approximately tetrahedral configuration to form two clusters (fig. 3). A new tetrahedral configuration forms from clusters in adjacent periods, and outgoing monopoles are shifted by $\beta/3$ and are either rotated by $\pi/3$ about the z -axis (for $W \in i\mathbb{R}$) or move back along the original directions (for $W \in \mathbb{R}$).

3.4 Higgs zeroes

As a further similarity with monopole scattering in \mathbb{R}^3 , we observe the appearance of an additional zero (termed an ‘antizero’ in [7]) during the $\ell = 0$ scattering process with $W \in \mathbb{R}$. The motion of Higgs zeroes can thus be described as follows: three zeroes move radially inwards on the vertices of an equilateral triangle, falling slightly below the plane $z = \beta/3$ as they approach. At some (C -dependent) value of W , a zero appears on the z axis, slightly above $\beta/3$ (fig. 4). Reducing W further, the zero splits into two, moving in the positive and negative z directions, fig. 5. At some value of W the downward-going zero (the antizero) meets the three original zeroes, resulting in the toroidal two-monopole cluster of fig. 3. However, the precise value of W at which this occurs is hard to resolve numerically. Details of the effect of varying C on the monopole structure will be presented in [11].

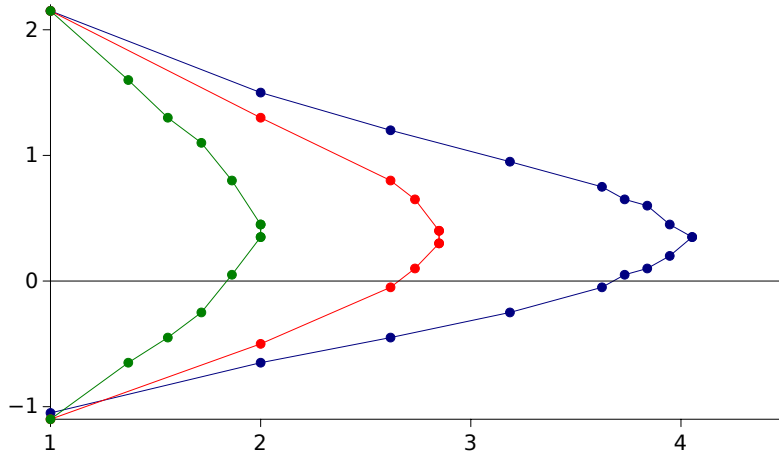


Figure 4: Motion of the zero-antzero pair along the z -axis (with 0 corresponding to $z = \beta/3$ and $\beta = 2\pi$) as a function of W for various values of C : $C = 1$ in blue (rightmost curve), $C = 2$ in red (middle) and $C = 5$ in green (left). For small C , the value of W at which the lower zero (the antzero) is centered at $z = \beta/3$ roughly coincides with the monopole closest to tetrahedral symmetry.

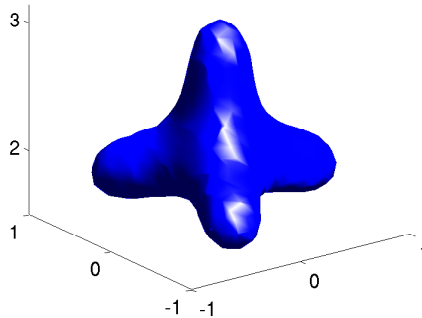


Figure 5: A contour of $\text{tr}(\hat{\Phi}^2)$ for the $C = 1$, $W = 2 + \sqrt{3}$ ($K = 4$) charge 3 solution of type $\ell = 1$. This shows the Higgs field is close to zero at the centre of the tetrahedron, although the energy density is not peaked there (fig. 3, but note the change of scale).

4 Multiplying chains

In this section we investigate how the Nahm data of a monopole chain can be constructed from that of a lower charge chain. This is possible when a chain can be described as a lower charge chain with a rescaled size C and period β . We will firstly consider a generalisation of the large N limit of the Ercolani-Sinha solution [12] given in [3]. Next, we will look at how charge $2k$ Nahm data with $\ell = k/2$ can be expressed as charge k Nahm data with $\ell = 0$, and suggest an interpretation.

4.1 Rescaling a charge 1 chain

Harland & Ward [3] considered a rescaling of the Nahm data relevant to a finite chain of N monopoles in the limit $N \rightarrow \infty$. In this limit, the Nahm data become infinite dimensional and operate on a k dimensional vector of functions. The $k \times k$ matrix corresponding to this action is the Nahm data of a periodic monopole. This procedure allowed the authors to reproduce the Nahm data of monopole chains of charge 1, and for the special charge 2 configuration consisting of a charge 1 chain of halved period. The resulting Nahm data is equivalent to that for $W = i$ on the submanifold Σ_2^1 . For higher charges, this procedure does not give a point on the surface Σ_k . For instance, in the charge 3 case we have

$$\Phi = \begin{pmatrix} 0 & e^{-\beta r/3} & e^{\beta(r/3+it)} \\ e^{\beta r/3} & 0 & e^{-\beta r/3} \\ e^{-\beta(r/3+it)} & e^{\beta r/3} & 0 \end{pmatrix} \quad A_{\bar{s}} = \frac{\beta}{6} \begin{pmatrix} 1 & 0 & 0 \\ 0 & 0 & 0 \\ 0 & 0 & -1 \end{pmatrix}. \quad (9)$$

This solution is of interest as the only currently known explicit solution with spectral curve coefficient $b_1 \neq 0$ (see section 2.2). In fact, the characteristic polynomial of Φ is $\zeta^3 - 3\zeta - (w + w^{-1}) = 0$. This is simply the $k = 3$ version of the spectral curve $\det(w - V_1(\zeta)^k) = 0$, where the holonomy of the charge 1 chain, $V_1(\zeta)$, is taken over k periods and satisfies $\text{tr}(V_1(\zeta)) = \zeta$ and $\det(V_1(\zeta)) = 1$. Note that $F = 0$, as expected for a charge 1 monopole chain (for which the Nahm data is of rank 1).

4.2 Embedding Nahm data

Another approach to construct higher charge chains is by embedding lower charge Nahm data along the diagonal of a higher rank matrix, with rescaled periods and a phase shift to ensure the resulting characteristic polynomial of Φ is a valid spectral curve. This construction will in general yield Nahm data of the wrong periodicity, although it can readily be cast into the standard form of section 3 by a change of gauge.

4.2.1 Charge k from charge 1

The charge 1 Nahm data is simply $\Phi^{(1)} = C \cosh(\beta s)$, $A^{(1)} = 0$. We form a traceless rank 2 Hitchin Higgs field by a phase shift of -1 , $\Phi' = C \cosh(\beta s/2)\sigma_3$. We should not be worried about the anti-periodicity of Φ' if we notice that it is periodic with period

$4\pi/\beta$, while the embedded charge 1 monopole has the dual period, $\beta/2$. Now we perform a non-periodic gauge transformation with

$$g = \frac{1}{\sqrt{2}} \begin{pmatrix} 1 & e^{i\beta t/2} \\ e^{-i\beta t/2} & -1 \end{pmatrix}$$

resulting in

$$\Phi^{(2)} = g^{-1} \Phi' g = C \cosh(\beta s/2) \begin{pmatrix} 0 & e^{i\beta t/2} \\ e^{-i\beta t/2} & 0 \end{pmatrix}$$

which is (up to a rescaling of C) the appropriate Hitchin Higgs field of a charge 2 chain, as can be obtained using the method of section 4.1. The gauge potential in the usual gauge is expected to be $A_{\bar{s}}^{(2)} = \beta\sigma_3/8$. Applying the inverse gauge transformation, we find that $A_{\bar{s}}^{(2)} = g^{-1} A'_{\bar{s}} g + g^{-1} \partial_{\bar{s}} g$ with $A'_{\bar{s}} = A_{\bar{s}}^{(1)}$. The structure of the inverse Nahm operator (1) relating the symmetries of ζ and z to those of Φ and A allows us to interpret the embedded charge 1 Nahm data as describing two monopoles of the same orientation (due to the rotational symmetry $(\zeta, z) \sim (-\zeta, z)$) but with z positions shifted by $\pm\beta/4$ from the origin (this is determined from (1) as twice the shift in $A_{\bar{s}}^{(1)}$ from $A_{\bar{s}}^{(1)} = 0$ for the single chain centered at $z = 0$).

An analogous procedure can be carried out to construct the charge 3 chain of section 4.1 from charge 1 Nahm data. This time we have

$$\Phi' = 2 \operatorname{diag} \left(\cosh \left(\frac{\beta s}{3} \right), \cosh \left(\frac{\beta s + 2i\pi}{3} \right), \cosh \left(\frac{\beta s - 2i\pi}{3} \right) \right), A_{\bar{s}} = \frac{\beta}{6} \operatorname{diag}(1, 0, -1)$$

which is gauge equivalent to (9) by conjugation with

$$g = \frac{1}{\sqrt{3}} \begin{pmatrix} 1 & e^{i\beta t/3} & e^{2i\beta t/3} \\ e^{-i\beta t/3 - 2i\pi/3} & 1 & e^{i\beta t/3 + 2i\pi/3} \\ e^{-2i\beta t/3 - 2i\pi/3} & e^{-i\beta t/3 + 2i\pi/3} & 1 \end{pmatrix}.$$

4.2.2 Charge 4 from charge 2

The same idea can be applied to higher charges. This allows us to take, say, a charge 2 monopole in pairs to give charge 4 Nahm data where the Higgs field is block-diagonal,

$$\Phi^{(4)} = \begin{pmatrix} \Phi^{(2)} & 0 \\ 0 & \Phi'^{(2)} \end{pmatrix},$$

which has a valid spectral curve as long as both $\Phi^{(2)}$ and $\Phi'^{(2)}$ have the same ℓ , with a relative overall phase of $e^{i\pi/2}$ and with K of opposite signs.

A special case is provided by $\Phi^{(2)}$ with $\ell = 0$ and $K = 0$. The gauge transformation

$$g = \frac{1}{\sqrt{2}} \begin{pmatrix} 1 & 0 & e^{i\beta t/2} & 0 \\ 0 & 1 & 0 & e^{i\beta t/2} \\ e^{-i\beta t/2} & 0 & -1 & 0 \\ 0 & ie^{-i\beta t/2} & 0 & -i \end{pmatrix}$$

shows that this is equivalent to the charge 4 case with $\ell = 2$ and $W = 1$ (see section 3.3.2). In other words, there are particular charge 4 configurations which can be understood as charge 2 chains “in disguise”, a result which could be anticipated by the \mathbb{Z}_4 symmetry of both cases.

The decoupling of the Nahm data into block-diagonal form suggests the relevant monopoles are ‘maximally separated’ and non-interacting. This is reminiscent of the decoupling of the moduli space metric of a charge 2 monopole into a direct product of two 1-monopole moduli space metrics for two well separated monopoles, [13, 14].

5 Conclusions

The work presented in this paper extends the construction of periodic monopoles of charge 1 and 2 to a particular family of higher charges. The resulting scattering processes correspond (in the small size to period ratio) to those scattering processes in \mathbb{R}^3 with cyclic symmetry [7], and it is clear how the number of different possibilities of a charge k monopole splitting into two clusters arises naturally from the structure of the Hitchin fields. We also consider a special case in which equally charged clusters are maximally separated, allowing the Nahm data to decouple and a description to be made in terms of lower charge monopoles.

There remain further geodesic submanifolds that do not fit the Ansatz (6). In particular, the search is still underway for solutions of the Hitchin equations with $b_1 \neq 0$ and $b_0 = 0$ (fig. 2), for which only the example (9) has been identified. A related question is whether one can construct a charge k ‘twisted chain’ of equally spaced monopoles invariant under a joint rotation and shift: $(\zeta, z) \sim (e^{i\pi/k}\zeta, z + m\beta/k)$ for $0 \leq m < k$. The existence of monopole chains with this symmetry has been established [15], but explicit periodic solutions are only available for $m = 0$ and $m = k/2$: they are the points on Σ_k^m with $K = 0$ ($W = \pm i$). For $m = 1$, $k = 3$ the spectral curve is expected to have $b_1 = b_0 = 0$ (central panel of fig. 2). It would be interesting to consider whether this solution can be described as a point on the geodesic containing the ‘tripled chain’ of section 4.1 and fig. 2.

6 Acknowledgements

Thanks to D.G. Harland for discussions and to R.S. Ward for use of the numerical procedure of [3]. This work was funded by an STFC studentship.

References

- [1] S. Cherkis, A. Kapustin, *Nahm Transform for Periodic Monopoles and $N=2$ Super Yang-Mills Theory*, Commun. Math. Phys. **218** (2001) 333, [arXiv:hep-th/0006050](#)
- [2] S.A. Cherkis, A. Kapustin, *Periodic Monopoles With Singularities And $N=2$ Super-QCD*, Commun. Math. Phys. **234** (2003) 1, [arXiv:hep-th/0011081](#)
- [3] D. Harland, R.S. Ward, *Dynamics of periodic monopoles*, Phys. Lett. **B 675** (2009) 262, [arXiv:0901.4428 \[hep-th\]](#)
- [4] R.S. Ward, *Periodic monopoles*, Phys. Lett. **B 619** (2005) 177, [arXiv:hep-th/0505254](#)
- [5] R. Maldonado, *Periodic monopoles from spectral curves*, JHEP02(2013)099, [arXiv:1212.4481 \[hep-th\]](#)
- [6] N.J. Hitchin, N.S. Manton, M.K. Murray, *Symmetric monopoles*, Nonlinearity **8** (1995) 661, [arXiv:dg-ga/9503016](#)
- [7] P.M. Sutcliffe, *Cyclic monopoles*, Nucl. Phys. **B 505** (1997) 517, [arXiv:hep-th/9610030](#)
- [8] R. Maldonado, R.S. Ward, *Geometry of Periodic Monopoles*, to appear in Phys. Rev. **D**, [arXiv:1309.7013 \[hep-th\]](#)
- [9] P.M. Sutcliffe, *Seiberg-Witten theory, monopole spectral curves and affine Toda solitons*, Phys. Lett. **B 381** (1996) 129, [arXiv:hep-th/9605192](#)
- [10] H.W. Braden, *Cyclic Monopoles, Affine Toda and Spectral Curves*, Commun. Math. Phys. **308** (2011) 303, [arXiv:1002.1216 \[math-ph\]](#)
- [11] R. Maldonado, *Scaling limits of periodic monopoles*, in preparation
- [12] N. Ercolani, A. Sinha, *Monopoles and Baker Functions*, Commun. Math. Phys. **125** (1989) 385
- [13] G.W. Gibbons, N.S. Manton, *The moduli space metric for well-separated BPS monopoles*, Phys. Lett. **B 356** (1995) 32
- [14] R. Bielawski, *Monopoles and Clusters*, Commun. Math. Phys. **284** (2008) 675, [arXiv:hep-th/0702190](#)
- [15] D.G. Harland, *Cyclic Monopole Chains*, to appear